Am J Physiol Heart Circ Physiol 297: H1697–H1710, 2009.
First published September 4, 2009; doi:10.1152/ajpheart.00595.2009.

Regulation of VASP phosphorylation in cardiac myocytes: differential regulation by cyclic nucleotides and modulation of protein expression in diabetic and hypertrophic heart

Juliano L. Sartoretto,[1] Benjamin Y. Jin,[1] Michael Bauer,[1] Frank B. Gertler,[2] Ronglih Liao,[1] and Thomas Michel[1]

[1]*Cardiovascular Division, Department of Medicine, Brigham and Women's Hospital, Harvard Medical School, Boston; and* [2]*Center for Cancer Research, Massachusetts Institute of Technology, Cambridge, Massachusetts*

Submitted 6 July 2009; accepted in final form 3 September 2009

Sartoretto JL, Jin BY, Bauer M, Gertler FB, Liao R, Michel T. Regulation of VASP phosphorylation in cardiac myocytes: differential regulation by cyclic nucleotides and modulation of protein expression in diabetic and hypertrophic heart. *Am J Physiol Heart Circ Physiol* 297: H1697–H1710, 2009. First published September 4, 2009; doi:10.1152/ajpheart.00595.2009.—Vasodilator-stimulated phosphoprotein (VASP) is a major substrate for cyclic nucleotide-dependent kinases that has been implicated in cardiac pathology, yet many aspects of VASP's molecular regulation in cardiomyocytes are incompletely understood. In these studies, we explored the role of VASP, both in signaling pathways in isolated murine myocytes, as well as in a model of cardiac hypertrophy in $VASP^{null}$ mice. We found that the β-adrenergic agonist isoproterenol promotes the rapid and reversible phosphorylation of VASP at Ser157 and Ser239. Forskolin and the cAMP analog 8-(4-chlorophenylthio)-cAMP promote a similar pattern of VASP phosphorylation at both sites. The effects of isoproterenol are blocked by atenolol and by compound H-89, an inhibitor of the cAMP-dependent protein kinase. By contrast, phosphorylation of VASP only at Ser239 is seen following activation of particulate guanylate cyclase by atrial natriuretic peptide, or following activation of soluble guanylate cyclase by sodium nitroprusside, or following treatment of myocytes with cGMP analog. We found that basal and isoproterenol-induced VASP phosphorylation is entirely unchanged in cardiomyocytes isolated from either endothelial or neuronal nitric oxide synthase knockout mice. In cardiomyocytes isolated from diabetic mice, only basal VASP phosphorylation is increased, whereas, in cells isolated from mice subjected to ascending aortic constriction (AAC), we found a significant increase in basal VASP expression, along with an increase in VASP phosphorylation, compared with cardiac myocytes isolated from sham-operated mice. Moreover, there is further increase in VASP phosphorylation in cells isolated from hypertrophic hearts following isoproterenol treatment. Finally, we found that $VASP^{null}$ mice subjected to transverse aortic constriction develop cardiac hypertrophy with a pattern similar to $VASP^{+/+}$ mice. Our findings establish differential receptor-modulated regulation of VASP phosphorylation in cardiomyocytes by cyclic nucleotides. Furthermore, these studies demonstrate for the first time that VASP expression is upregulated in hypertrophied heart.

signal transduction; endothelial nitric oxide synthase; neuronal nitric oxide synthase; phosphoprotein

VASODILATOR-STIMULATED PHOSPHOPROTEIN (VASP) is the archetypal member of a family of actin-binding proteins termed the ENA/VASP protein family (34). This protein family includes the Drosophila protein Enabled (ENA), its mammalian homolog MENA, the ENA/VASP-like protein Evl, and VASP (13). MENA/VASP proteins are implicated in actin polymerization, and these proteins appear to modulate diverse cellular responses, including cell migration (26). VASP was initially isolated from human platelets (15, 16), and the protein has been extensively characterized as a substrate for cAMP- and cGMP-dependent protein kinases (40). Three phosphorylation sites (serine 157, serine 239, and threonine 278) have been identified in human VASP (38, 39). Ser157 is the preferred site for phosphorylation by the cAMP-dependent protein kinase (PKA), whereas Ser239 is the site preferentially phosphorylated by the cGMP-dependent protein kinase (PKG) (38, 39). Thr278 has recently been shown to be phosphorylated by the AMP-activated protein kinase (4). In different cell types, VASP phosphorylation pathways have been implicated in diverse cellular responses, ranging from endothelial cell permeability and angiogenesis (7, 8) to platelet aggregation and secretion (1, 2). Although VASP phosphorylation pathways have been extensively investigated in blood platelets and vascular smooth muscle cells, little is known about the modulation of VASP phosphorylation in the heart. Since abnormalities in cyclic nucleotide-modulated signaling pathways have been implicated in cardiomyopathy and heart failure (29), we decided, first, to explore the regulation of VASP phosphorylation in healthy mouse cardiac myocytes, and, second, to investigate whether VASP plays a role in the stressed heart.

In the normal mammalian heart, VASP expression appears to be enriched at the intercalated disks at the cell-cell boundaries between cardiac myocytes (12). However, mice with targeted deletion of VASP do not appear to show obvious developmental defects in cardiac structure or function (19), yet more detailed analyses of cardiac function in the VASP knockout mouse have not been reported. Transgenic mice overexpressing a dominant-negative VASP mutant in the heart develop a dilated cardiomyopathy and myocyte hypertrophy, associated with early postnatal lethality (10). Transgenic mice overexpressing the dominant-negative VASP mutant showed a displacement of both VASP and MENA from cardiac intercalated disks, suggesting that disruption of intercellular contacts in these transgenic mouse hearts contributes to their cardiac dysfunction (20, 21).

Little is known about VASP phosphorylation pathways in cardiac myocytes, despite the presence of diverse receptor-activated pathways that modulate the activation of adenylate and guanylate cyclases in these cells. In cardiac myocytes, cGMP is synthesized by two distinct guanylate cyclase isoforms: the soluble guanylate cyclase (sGC) isoform, which is

Address for reprint requests and other correspondence: T. Michel, Brigham and Women's Hospital, Cardiovascular Division, Thorn Bldg., Rm. 1210A, 75 Francis St., Boston, MA 02115 (e-mail: thomas_michel@harvard.edu).

activated by nitric oxide (NO), and the particulate guanylate cyclase, which is activated by binding atrial natriuretic peptide (ANP) (17, 25, 30). Both the endothelial (eNOS) and neuronal NO synthase (nNOS) isoforms are expressed in cardiac myocytes, and these cells are also responsive to extracellular NO from endothelial cells (coronary arteries) or from pharmacological sources of NO (11, 41). Of the multiple G protein-coupled receptors that lead to adenylate cyclase activation in cardiac myocytes, perhaps the best characterized is the β-adrenergic receptor pathway, which represents the archetypal pathway leading to cAMP accumulation in the heart. In these studies, we have explored the agonist-modulated pathways that regulate VASP phosphorylation in normal adult murine cardiac myocytes. We have also investigated VASP expression and phosphorylation in cardiac myocytes isolated from wild-type, diabetic (*db/db*), and VASP^{null} mice studied following aortic constriction in a cardiac hypertrophy model.

EXPERIMENTAL PROCEDURES

Materials. Polyclonal antibodies directed against phospho-VASP (Ser157 and Ser239), total VASP, MENA, phospho-eNOS (Ser1177), and Akt were from Cell Signaling Technologies (Beverly, MA). Total eNOS monoclonal antibody was from BD Transduction Laboratories (Lexington, KY). Collagenase type 2 was from Worthington Biochemical (Lakewood, NJ). Super Signal substrate for chemiluminescence detection and secondary antibodies conjugated with horseradish peroxidase were from Pierce. Tris-buffered saline and phosphate-buffered saline were from Boston Bioproducts (Ashland, MA). Laminin was from BD Bioscience (San Jose, CA). Minimum essential medium with Hank's balanced salt solution and glutamine were from Gibco-BRL. Calf serum was from HyClone (Logan, UT). Isoflurane was from Abbott (North Chicago, IL). Heparin sodium was from APP (Los Angeles, CA). Pentobarbital sodium was from Ovation Pharmaceutics (Deerfield, IL). Forskolin, 1*H*-[1,2,4]oxadiazolo[4,3-*a*]quinoxalin-1-one (ODQ), and H-89 were from Calbiochem. 8-CTP-cAMP-AM was from BioLog (Germany). All other reagents were from Sigma (Plymouth Meeting, PA). Mouse lines were from Jackson Laboratories (Bar Harbor, ME) [wild type (C57B16/J), eNOS^{null} (B6.129P2-Nos3), nNOS^{null} (B6;129S4-Nos1), and diabetic (B6.Cg-m+/+Lepr^{db}/J)]; VASP^{null} mice were previously generated and characterized (2).

Aortic constriction. Constriction of the transverse and ascending thoracic aorta was performed on 9-wk-old male mice. In brief, mice were anesthetized, intubated, and placed on a respirator. Midline sternotomy was performed, the aorta was visualized, and a suture was placed around the aorta distal to the brachiocephalic artery (transverse) and ascending aorta (ascending). The suture was tightened around a blunt 27-gauge needle placed adjacent to the aorta. The needle was then removed, and the chest and overlying skin were closed. After 2 and 5 wk, echocardiography was performed on awake mice to evaluate cardiac function. Sham-operated mice littermates were used as controls.

Blood pressure. Tail-cuff method blood pressure (BP) was measured in unanesthetized animals by an indirect tail-cuff method (2000 Blood Pressure Analysis program). Mice were acclimated to the ambient conditions in the testing room for at least 20 min, and then three consecutive measurements of BP were determined and averaged.

Isolation of adult mouse ventricular myocytes. All animal experimentation was performed according to protocols approved by the Harvard Medical School Committee on Use of Animals in Research. Cardiac myocyte isolation methods basically followed the procedures as described (33), with modifications as noted. For these studies, 8- to 10-wk-old, wild-type, gene-targeted eNOS (eNOS$^{-/-}$) and nNOS (nNOS$^{-/-}$), diabetic (*db/db*), VASP^{null}, or wild-type mice with transverse aortic constriction (TAC) were anesthetized with isoflurane, heparinized, and then injected with lethal dose of pentobarbital sodium. The heart was quickly removed from the chest and retrogradely perfused through the aorta, as described (35). The procedure for cardiac myocyte isolation followed the protocol described in detail in Ref. 35. In brief, enzymatic digestion was initiated by adding collagenase type 2 to the cardiac perfusion solution, followed by the stepwise introduction of $CaCl_2$, after which the heart tissue was minced, and the cells were dispersed by trituration, following which the cardiac myocytes were allowed to settle and then were washed, pelleted, counted, and plated.

Cell culture. Cardiac myocytes were plated in laminin-coated 60-mm culture dishes (200,000 rod-shaped cells per dish) in medium consisted of minimum essential medium with Hank's balanced salt solution and supplemented with calf serum (10% vol/vol), 2,3-butanedione monoxime (10 mM), penicillin-streptomycin (100 U/ml), glutamine (2 mM), and ATP (2 mM). After the cells attached to the dish (~1 h), the plating medium was changed to minimum essential medium with Hank's balanced salt solution, supplemented with bovine serum albumin (1 mg/ml), penicillin-streptomycin (100 U/ml), and glutamine (2 mM). Cell treatments were performed after culturing the cells for 4 h.

Genotyping. VASP^{null} mice have been previously generated and characterized (2). Heterozygous mice were crossed to generate litters consisting of VASP$^{+/+}$ (wild-type controls) and VASP^{null} knockout animals. The pups were genotyped by PCR as described (2): VASP^{null} mice were detected using the forward primer 5′-TGC CTA TCT GTT CAC AAC ATG G-3′ and a reverse primer 5′-AAA CGA TCA CAG TAG CCC G-3′ to generate a 600-bp product. Detection of VASP$^{+/+}$ mice used the forward primer 5′-TGC CTA TCT GTT CAC AAC ATG G-3′ and reverse primer 5′-GGT TAC GTT GGT GTA GAT GGG-3′ to yield a 350-bp product.

Western blots. After drug treatments, cardiac myocytes were washed with phosphate-buffered saline and incubated on ice for 20 min in lysis buffer (50 mM Tris·HCl, pH 7.4, 150 mM NaCl, 1% Nonidet P-40, 0.25% sodium deoxycholate, 1 mM EDTA, 2 mM Na_3VO_4, 1 mM NaF, 2 μg/ml leupeptin, 2 μg/ml antipain, 2 μg/ml soybean trypsin inhibitor, and 2 μg/ml lima trypsin inhibitor). Cells were harvested by scraping and then rotated for 15 min at 4°C. For immunoblot analyses, 50 μg of cellular protein were resolved by SDS-PAGE. After separation by SDS-PAGE, proteins were electroblotted onto nitrocellulose membranes. After incubating the membranes in 5% nonfat dry milk in Tris-buffered saline with 0.1% (vol/vol) Tween 20 (TBST), membranes were incubated overnight in TBST containing 5% bovine serum albumin plus the specified primary antibody. After four washes (10 min each) with TBST containing 1% milk, the membranes were incubated for 1 h with a horseradish peroxidase-labeled goat anti-rabbit or anti-mouse immunoglobulin secondary antibody in TBST containing 1% milk. The membranes were washed four additional times in TBST containing 1% milk, then incubated with a chemiluminescent reagent, according to the manufacturer's protocols (SuperSignal West Femto), and digitally imaged in a chemiluminescence imaging system (Alpha Innotech, San Leandro, CA). Quantitative analyses of the chemiluminescent signals were performed using an AlphaEase FC software (Alpha Innotech, San Leandro, CA). Where indicated in the experiments showing quantitative densitometry of Western blots, the ordinate is in arbitrary units.

Statistical analysis. All experiments were performed at least three times. Mean values for individual experiments were expressed as means ± SE. Statistical differences were assessed by ANOVA or *t*-test, as indicated. A P value of <0.05 was considered significant.

RESULTS

Isoproterenol-stimulated VASP phosphorylation in adult murine cardiac myocytes. Adult mouse cardiac myocytes were isolated, treated with the adrenergic agonist isoproterenol,

harvested, and analyzed in immunoblots, as described above. Figure 1*A* presents the results of immunoblot analyses exploring the time course of isoproterenol-induced phospho-VASP; the immunoblots were probed with selective antibodies, as shown. Note that phosphorylation of VASP on Ser157 leads to a shift in apparent molecular mass in SDS-PAGE from 46 to 50 kDa, as previously reported (17). Following the addition of isoproterenol (1 μM) to adult murine cardiac myocytes, phos-

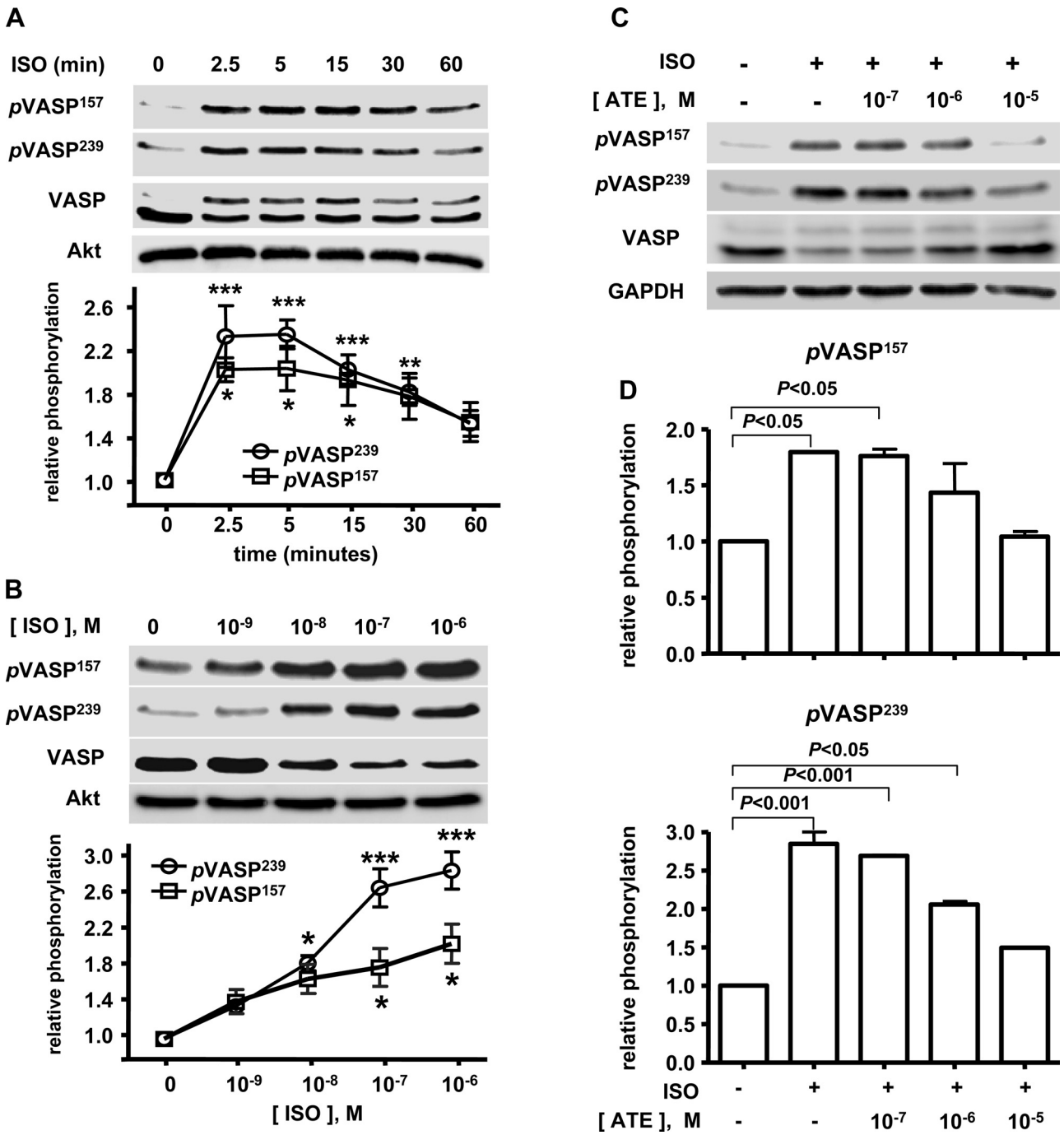

Fig. 1. Time-concentration responses for isoproterenol (ISO)-mediated vasodilator-stimulated phosphoprotein (VASP) phosphorylation and β_1-adrenergic receptor blockade effect on ISO-induced VASP phosphorylation. Shown are the results of immunoblots analyzed in lysates prepared from adult murine cardiac myocytes treated with ISO (100 nM) for the indicated times (*A*) or concentrations (*B*; 5-min incubation with ISO), and treated with the β_1-adrenergic antagonist atenolol (ATE) at the indicated concentrations and then treated with ISO (*C*; 100 nM for 5 min). Cell lysates were analyzed in immunoblots probed using antibodies directed against phospho-VASP (pVASP) Ser157, pVASP Ser239, total VASP, Akt, and GAPDH, as indicated. The experiment shown is representative of three independent experiments that yielded similar results. Below each immunoblot are the results of densitometric analyses from pooled data, showing the fold increase in VASP phosphorylation (in arbitrary units) in cardiac myocytes treated with ISO at the indicated times (*A*), ISO concentrations (*B*), or ATE concentrations (*D*) plotted relative to the signals present in unstimulated cells. Each data point represents the mean ± SE derived from three independent experiments. The results are significant at the $P < 0.05$ level. $^*P < 0.05$, $^{**}P < 0.01$, and $^{***}P < 0.001$ for VASP phosphorylation vs. unstimulated cells (ANOVA).

phorylation of VASP at Ser157 and Ser239 rapidly and markedly increases, reaching a maximum response at 5 min, and slowly returning to baseline (Fig. 1*A*). This response is statistically significant. We next determined the isoproterenol dose response for VASP phosphorylation in these cells (Fig. 1*B*): mouse cardiac myocytes were treated for 5 min with varying concentrations of isoproterenol and analyzed in immunoblots probed with antibodies directed either against total VASP or with phosphospecific VASP antibodies, and with antibody directed against total Akt as loading control. Figure 1, *top*, shows immunoblot data from representative experiments; the *bottom* panels present the results of densitometric analyses of pooled data, which reveal that isoproterenol-stimulated VASP phosphorylation at Ser157 and Ser239 has an EC_{50} of ~10 nM.

Effects of the β-adrenergic antagonist atenolol on isoproterenol-promoted VASP phosphorylation. Figure 1*C* shows the results of immunoblot analyses performed in adult cardiac myocyte lysates prepared from cells incubated with the β-adrenergic antagonist atenolol at the indicated concentrations before treatment with isoproterenol. Immunoblots were probed with antibodies directed against phospho-VASP Ser157, phospho-VASP Ser239, total VASP, and GAPDH, as indicated. Figure 1*D* presents pooled data from three independent experiments analyzed by quantitative chemiluminescence of immunoblots. As can be seen in this figure, atenolol blocks isoproterenol-promoted VASP phosphorylations, with an IC_{50} of ~1 μM.

cAMP and isoproterenol-promoted VASP phosphorylation. We used pharmacological activators and inhibitor to explore the involvement of the cAMP/PKA pathway in VASP phosphorylation in cardiac myocytes (Fig. 2). In this figure, *A*, *C*, and *E* show the results of representative immunoblots, and *B*, *D*, and *F* show the results of densitometric analyses of pooled data for phosphorylation of VASP at Ser157 and Ser239. As shown in Fig. 2, *A* and *B*, the adenylate cyclase activator forskolin promotes VASP phosphorylation to a magnitude similar to that seen with isoproterenol, as does the cAMP analog, 8-(4-chlorophenylthio)adenosine-3',5'-cyclic monophosphate, acetoxymethyl ester (8-CPT-cAMP-AM) (Fig. 2, *C* and *D*). When cells are first treated with the PKA inhibitor

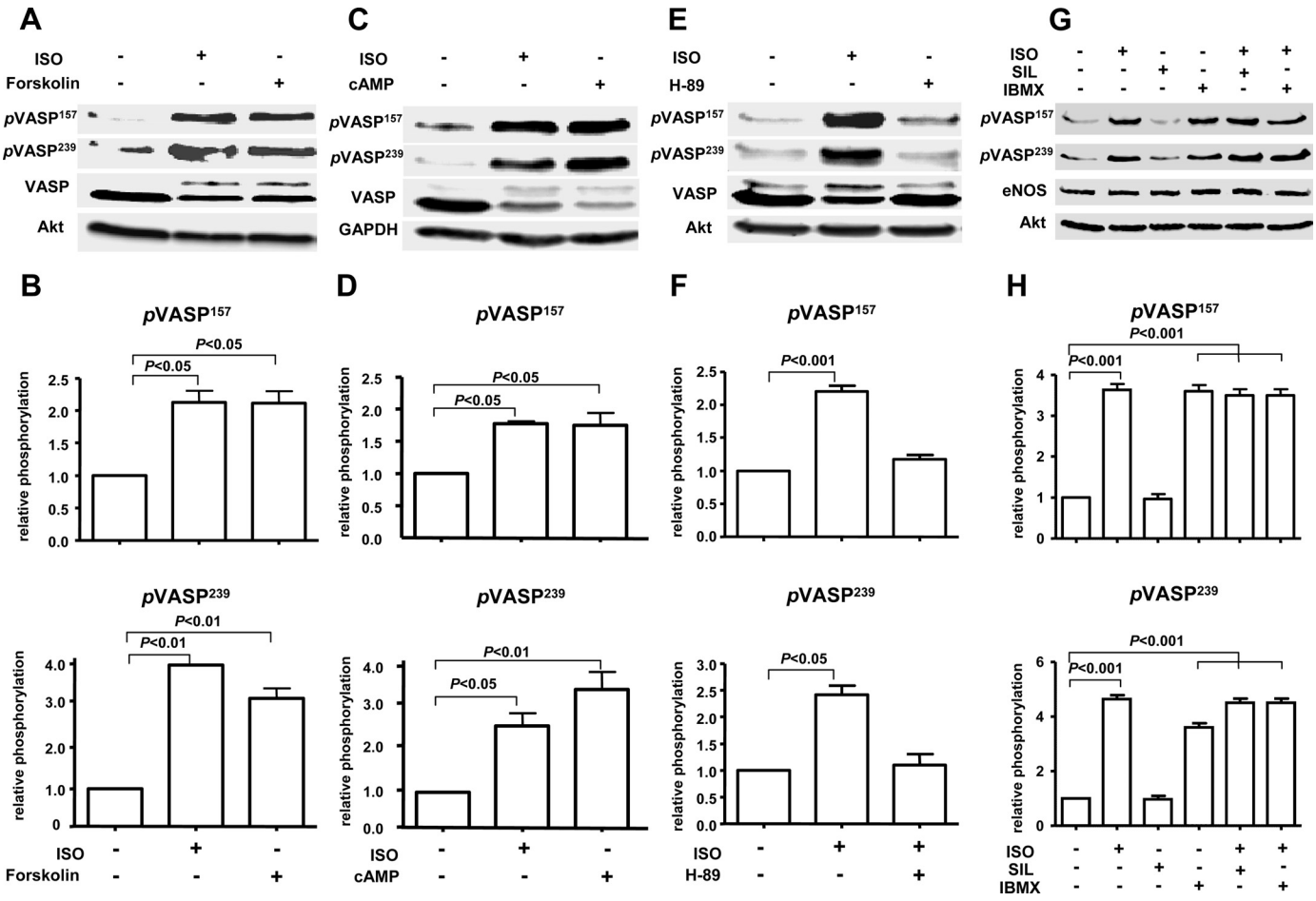

Fig. 2. Effects of the adenylate cyclase/cAMP/PKA pathway on VASP phosphorylation in cardiac myocytes. *A*, *C*, *E*, and *G*: results of immunoblots analyzed in lysates prepared from cardiac myocytes isolated from adult mice treated with ISO (100 nM, 5 min), forskolin (10 μM, 5 min), 8-(4-chlorophenylthio)adenosine-3′,5′-cyclic monophosphate acetoxymethyl ester (8-CPT-cAMP-AM; 10 μM, 5 min), PKA inhibitor H-89 (10 μM, 30 min), sildenafil (SIL; 20 μM, 30 min), or 3-isobutyl-1-methylxanthine (IBMX; 1 mM, 30 min). Cell lysates were analyzed in immunoblots probed using antibodies directed against pVASP Ser157, pVASP Ser239, total VASP, Akt, or GAPDH, as indicated. The experiment shown is representative of three independent experiments each that yielded similar results. *B*, *D*, *F*, and *H*: results of densitometric analyses from pooled data, plotting the fold increase in VASP phosphorylation (in arbitrary units) relative to the signals present in unstimulated cells. Each data point represents mean ± SE derived from three independent experiments. The results are significant at the $P < 0.05$ level (ANOVA). eNOS, endothelial nitric oxide synthase (NOS).

compound H-89, subsequent isoproterenol-induced VASP phosphorylation is abrogated (Fig. 2, *E* and *F*). The nonselective phosphodiesterase (PDE) inhibitor 3-isobutyl-1-methylxanthine (IBMX), but not the PDE-5-selective inhibitor sildenafil, promoted a significant increase in VASP phosphorylation; in the presence of IBMX, addition of isoproterenol yields no additional VASP phosphorylation, (Fig. 2, *G* and *H*).

VASP phosphorylation and NO signaling. Our laboratory and others have previously reported that isoproterenol promotes activation of NOS in cardiac myocytes (3, 22), associated with changes in cyclic nucleotide signaling pathways. As shown in Fig. 3, *A* and *B*, we found that isoproterenol treatment of adult mouse cardiac myocytes promotes the phosphorylation of eNOS at Ser1177, a phosphorylation site associated with enzyme activation (28). The addition of isoproterenol to mouse cardiac myocytes promotes the rapid (Fig. 3*A*) and potent (Fig. 3*B*) phosphorylation of eNOS at Ser1177. The maximal response for isoproterenol-induced eNOS phosphorylation is seen at 15 min, with an EC_{50} of ~10 nM. We found that the NOS inhibitor N^G-nitro-L-arginine methyl ester (L-NAME) has no effect on isoproterenol-promoted VASP phosphorylation (Fig. 3, *C* and *D*). Similarly, the soluble guanylate inhibitor ODQ does not alter isoproterenol-promoted VASP phosphorylation in cardiac myocytes (Fig. 3, *E* and *F*). To further explore the role of NO pathways in isoproterenol-induced phospho-VASP, we analyzed responses in cardiac myocytes isolated from NOS gene-targeted mice. Figure 4, *A* and *B*, shows the results of immunoblots analyzed in cardiac myo-

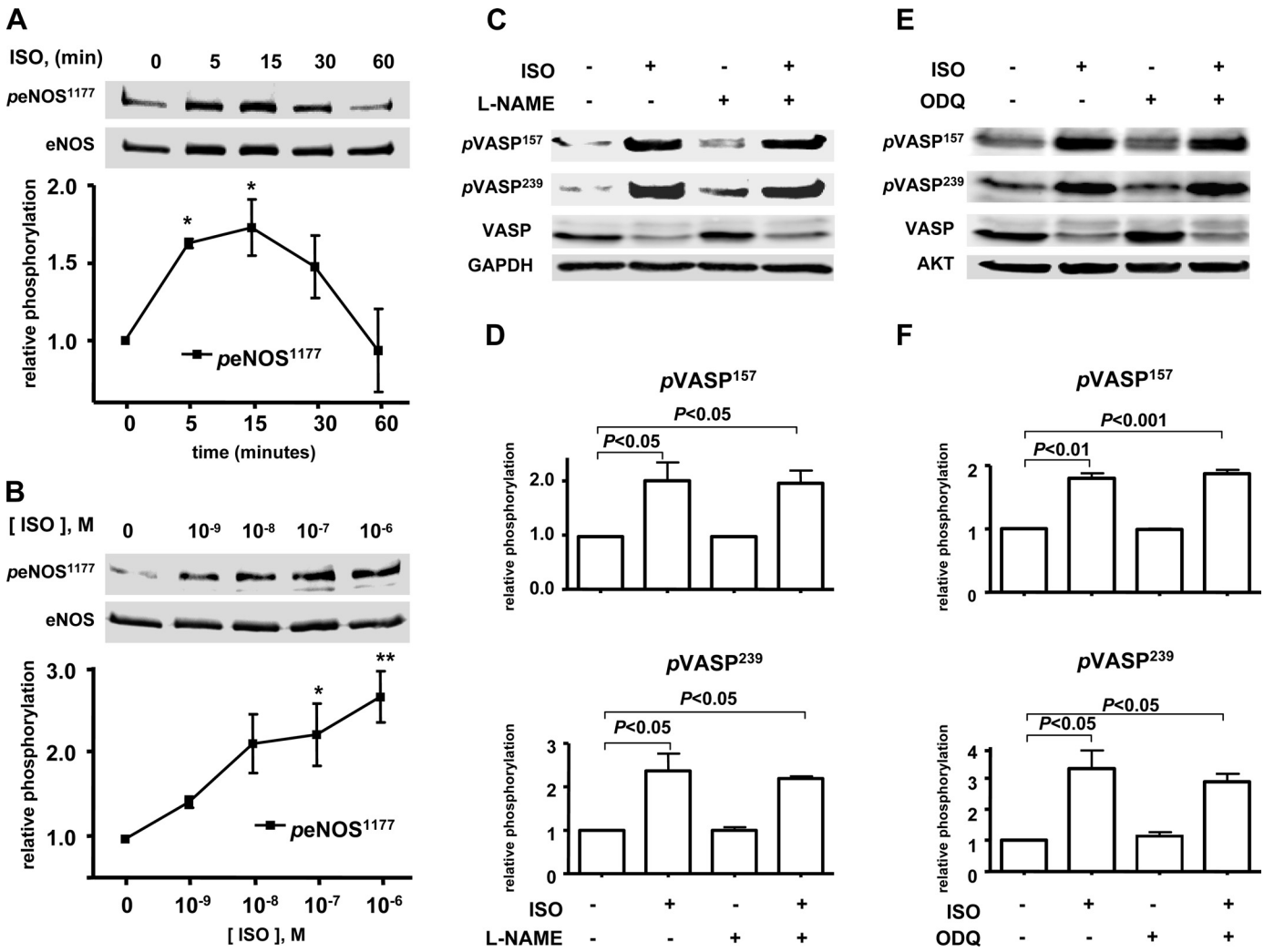

Fig. 3. Time concentration response for ISO-mediated eNOS phosphorylation at Ser1177 and the effects of NOS or guanylate cyclase inhibitor on ISO-induced VASP phosphorylation. This figure shows the results of time course (treated with 100 nM isoproterenol; *A*) and dose-response (treated with ISO for 5 min; *B*) experiments for ISO-stimulated eNOS Ser1177 phosphorylation in murine cardiac myocytes. *C* and *E*: results from cardiac myocytes incubated either with N^G-nitro-L-arginine methyl ester (L-NAME; 1 mM, 30 min) or with soluble guanylate cyclase inhibitor 1*H*-[1,2,4]oxadiazolo[4,3-*a*]quinoxalin-1-one (ODQ; 10 μM, 30 min), respectively, and then treated with ISO (100 nM, 5 min). Cell lysates were resolved by SDS-PAGE and probed using antibodies directed against phospho-eNOS (peNOS) Ser1177, total eNOS, pVASP Ser157, pVASP Ser239, total VASP, Akt, and GAPDH, as indicated. The experiment shown is representative of three independent experiments that yielded similar results. Below each immunoblot is shown the results of densitometric analyses from pooled data, plotting the fold increase of the degree of phosphorylation (in arbitrary units) of eNOS at the times (*A*) and concentrations (*B*) indicated, relative to the signals present in unstimulated cardiac myocytes. Each data point represents the mean ± SE derived from three independent experiments. $*P < 0.05$ and $**P < 0.01$ for eNOS phosphorylation vs. unstimulated cells (ANOVA). *D* and *F*: results of densitometric analyses from pooled data, plotting the fold increase in VASP phosphorylation relative to the signals present in the untreated cells. Each data point represents the mean ± SE derived from three independent experiments (ANOVA).

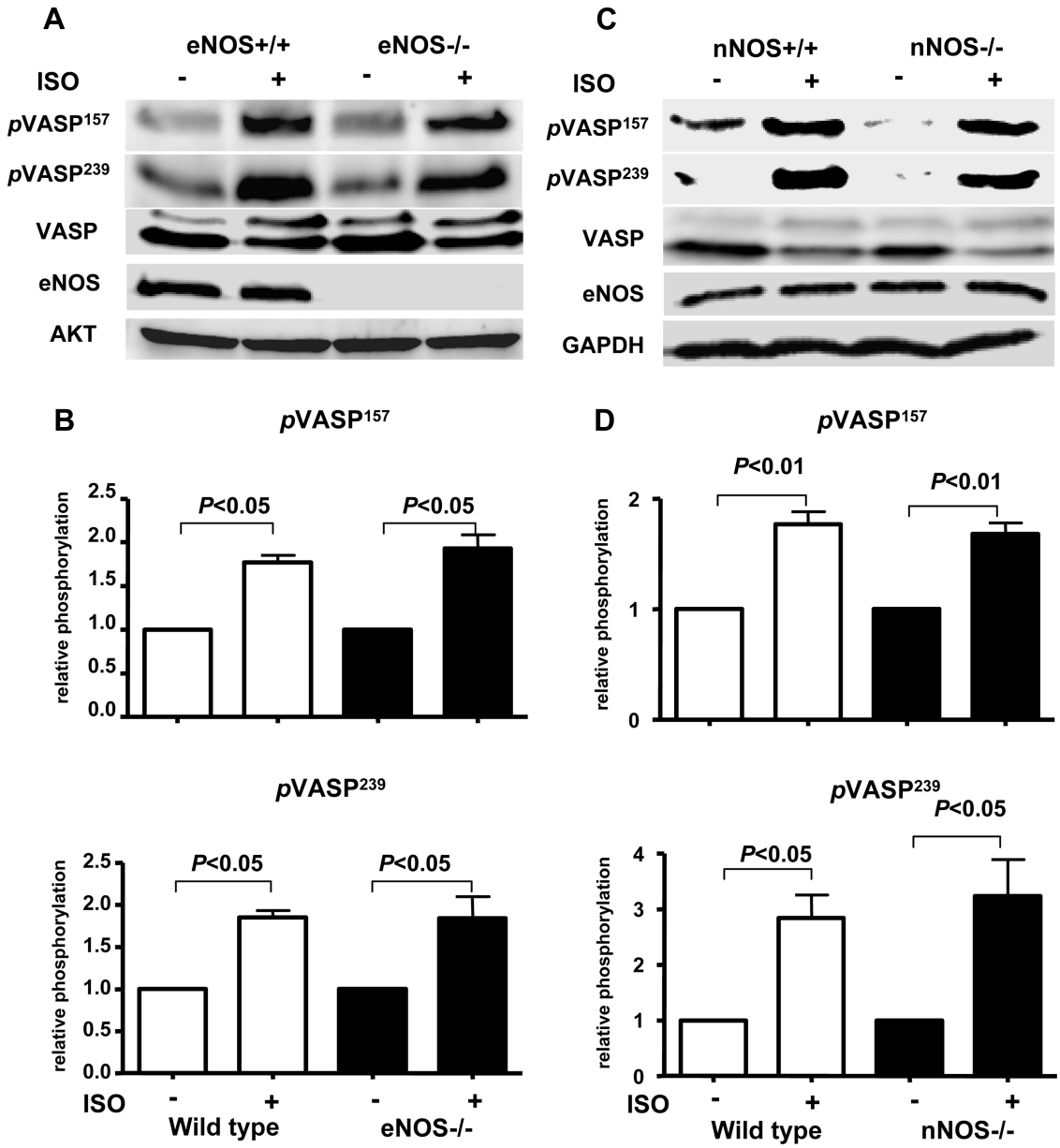

Fig. 4. Isoproterenol-induced VASP phosphorylation in cardiac myocytes isolated from eNOS or neuronal NOS (nNOS) knockout mice. This figure shows results of immunoblots analyzed in lysates prepared from cardiac myocytes isolated from wild-type, endothelial ($eNOS^{null}$), or neuronal ($nNOS^{null}$) NOS knockout adult mice and treated with ISO (100 nM, 5 min). Cell lysates were resolved by SDS-PAGE and probed using antibodies directed against pVASP Ser157, pVASP Ser239, total VASP, eNOS, Akt, or GAPDH, as indicated. *A* and *C*: experiment shown are representative of three independent experiments each that yielded similar results. *B* and *D*: results of densitometric analyses from pooled data, plotting the fold increase in VASP phosphorylation relative to the signals present in the untreated cells. Each data point represents the mean ± SE derived from three independent experiments (ANOVA).

cytes treated with isoproterenol after isolation from $eNOS^{-/-}$ and wild-type mice and probed with antibodies directed against Ser157, Ser239 phospho-VASP, total VASP, eNOS, and Akt. Isoproterenol-promoted VASP phosphorylation is unaltered in cardiac myocytes isolated from the $eNOS^{-/-}$ mouse compared with the wild-type myocytes (Fig. 4, *A* and *B*). We then performed analogous experiments using cardiac myocytes isolated from nNOS knockout mice (Fig. 4, *C* and *D*). As found for the $eNOS^{-/-}$ mouse, the pattern of isoproterenol-promoted phospho-VASP did not differ between the $nNOS^{-/-}$ and wild-type cardiomyocytes.

Guanylate cyclase activation and VASP phosphorylation. Although cardiac myocytes from both the $eNOS^{-/-}$ and $nNOS^{-/-}$ mice showed no substantive changes in VASP phosphorylation (Fig. 4), we still sought to explore whether an exogenous source of NO might activate sGC in these cells. Treatment of murine cardiac myocytes with the NO-donating drug sodium nitroprusside (SNP) showed a striking increase in phosphorylation of VASP at Ser239, with no effect on phosphorylation at Ser157 (Fig. 5, *A* and *B*). The SNP response was completely blocked by the sGC inhibitor ODQ (Fig. 5*C*). We also explored additional features of ANP-promoted VASP

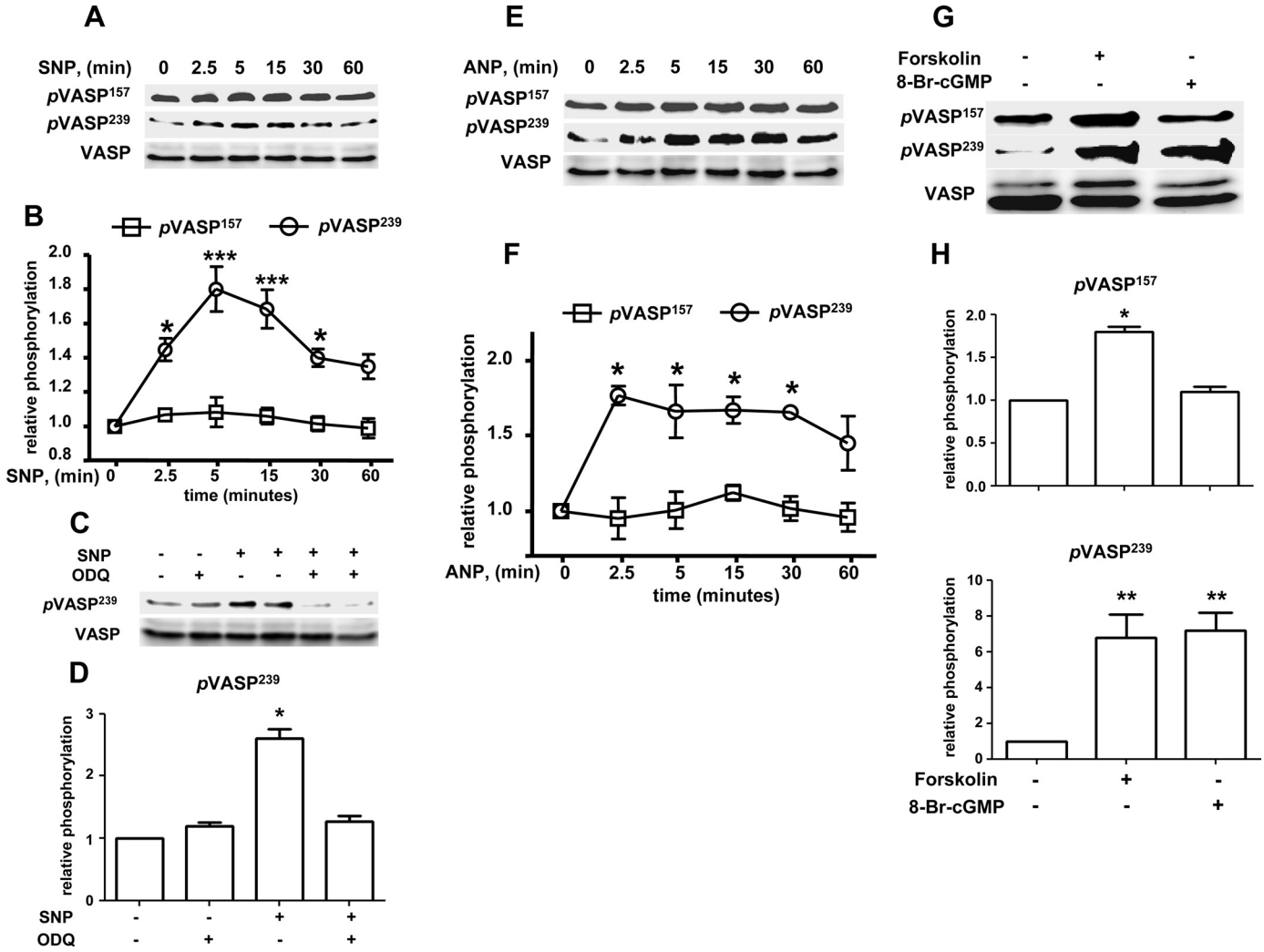

Fig. 5. Sodium nitroprusside (SNP) or atrial natriuretic peptide (ANP) promotes phosphorylation of VASP Ser239 in cardiac myocytes. This figure shows results of immunoblots analyzed in lysates prepared from isolated murine cardiac myocytes treated with SNP (1 μM) for the indicated times. *A*: cells treated with the soluble guanylate cyclase inhibitor ODQ (10 μM, 30 min) and then incubated with SNP (1 μM, 5 min). *C*: cells treated with ANP (1 μM) for the indicated times. Results are shown of cells treated with forskolin (10 μM, 5 min; *E*) or 8-bromo-cGMP (8-Br-cGMP; 200 μM, 15 min; *G*). Cell lysates were resolved by SDS-PAGE and probed using antibodies directed against pVASP Ser157, pVASP Ser239, or total VASP, as shown. *B*, *D*, *F*, and *H*: results of densitometric analyses from pooled data, plotting the fold increase in VASP phosphorylation relative to the signals present in unstimulated cells. Each data point represents the mean ± SE derived from three independent experiments. $*P < 0.05$, $**P < 0.01$, and $***P < 0.001$ for pVASP239 vs. unstimulated cells (ANOVA). The experiment shown is representative of three independent experiments that yielded similar results.

phosphorylation. As shown in Fig. 5, *D* and *E*, ANP treatment promotes the rapid phosphorylation of VASP on Ser239, but has no effect on phosphorylation at Ser157. There was no effect of ODQ on ANP-promoted VASP phosphorylation (data not shown). We then performed an experiment in which cardiac myocytes were either treated with forskolin or cGMP-dependent protein kinase activator 8-bromo-cGMP. As shown in Fig. 5*F*, activation of cGMP-dependent kinases promotes phosphorylation of VASP at Ser239 only. Stimulation either of sGC (SNP) or of particulate guanylate cyclase (ANP) leads to VASP phosphorylation at Ser239. However, in contrast to the response elicited by isoproterenol, activation of cGMP pathways by NO or ANP does not promote VASP phosphorylation at Ser157.

VASP phosphorylation in cardiac myocytes isolated from db/db diabetic mice. Because of the postulated involvement of cyclic nucleotide signaling pathways in diabetic cardiomyopathy, we analyzed VASP expression and phosphorylation responses in cardiac myocytes isolated from *db/db* obese diabetic mice. As shown in Fig. 6, there is no change in the overall level of VASP expression in cardiac myocytes isolated from *db/db* mice compared with nonobese *db/+* littermates, normalized either to the abundance of actin or PKA in these samples. However, there is a marked increase in the basal levels of VASP phosphorylation at Ser157 and Ser239 sites. The striking increase in VASP phosphorylation in cardiac myocytes isolated from the *db/db* mouse was not significantly affected by the addition of isoproterenol to cells. In contrast, isoproterenol treatment of the nonobese *db/+* littermates showed an increase in VASP phosphorylation at both Ser157 and Ser239, starting from a lower basal phosphorylation level. Importantly, treatment of cardiac myocytes isolated from the *db/db* mice with the PKA inhibitor H-89 completely reversed the increase in VASP phosphorylation seen in the diabetic animals (Fig. 6*C*),

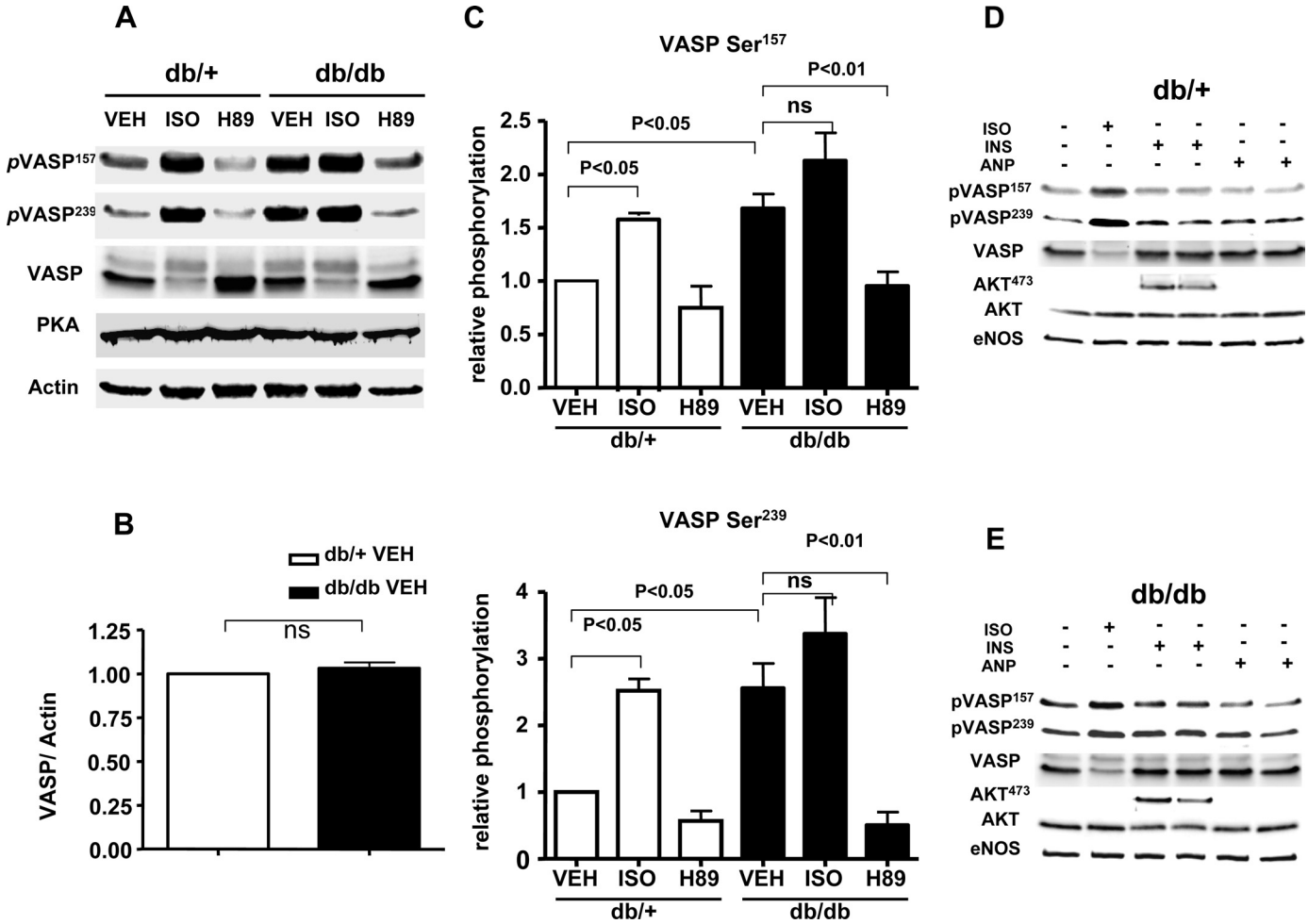

Fig. 6. VASP phosphorylation in cardiac myocytes isolated from *db/db* obese diabetic mice. This figure shows results of immunoblots analyzed in lysates prepared from cardiac myocytes isolated from *db/db* obese diabetic mice or their wild-type littermates (*db*/+), lean nondiabetic mice, and treated either with ISO (100 nM for 5 min) or H-89 (10 μM for 30 min). *A*: cell lysates were resolved by SDS-PAGE and probed using antibodies directed against pVASP Ser157, pVASP Ser239, total VASP, actin, or PKA, as indicated. The experiment is representative of five independent experiments that yielded similar results. *B*: results of densitometric analyses from pooled data, plotting the total VASP (no treatment) abundance relative to actin abundance. Each data point represents the mean ± SE derived from five independent experiments (*t*-test). *C*: the results of densitometric analyses from pooled data, plotting the fold increase in pVASP Ser157 or Ser239 relative to the signals present in untreated cells. *D* and *E*: results of immunoblots analyzed in lysates prepared from cardiac myocytes isolated from *db/db* obese diabetic mice (*E*) or their wild-type littermates (*db*/+; *D*) and treated with ISO (100 nM for 5 min), insulin (INS; 1 μM for 15 min), or ANP (1 μM for 15 min). Each data point represents the mean ± SE derived from five independent experiments (ANOVA). VEH, vehicle.

without any accompanying change in expression of PKA (Fig. 6*A*). As shown in Fig. 6, *D* and *E*, neither insulin nor ANP promote any substantive change in VASP phosphorylation Ser157 in either *db*/+ or *db/db* cardiocytes. Both ANP and insulin promote a small but reproducible increase in phosphorylation of VASP residue Ser239 in cardiocytes isolated either from the *db/db* diabetic or *db*/+ nondiabetic mouse; insulin-dependent activation of kinase Akt in cardiac myocytes is equally robust in both lines.

VASP phosphorylation in cardiac myocytes isolated from mice subjected to AAC. Since cardiac myocyte hypertrophy involves changes in the cardiac actin cytoskeleton, and since the role of the actin-binding protein VASP in myocyte hypertrophy is unknown, we expanded our work to analyze VASP/MENA expression, along with VASP phosphorylation responses in cardiac myocytes isolated from wild-type mice (C57BL/6) subjected to AAC. As shown in Fig. 7, *D*, *E*, and *F*, following AAC, there is a significant increase in basal MENA and VASP expression, with a commensurate increase in VASP phosphorylation, as normalized to the abundance of either GAPDH or actin; sham-operated mice serve as a control. The marked increase in VASP phosphorylation in cardiac myocytes isolated from hypertrophic heart was further affected by the addition of isoproterenol to the cells (Fig. 8). The mice subjected to AAC developed significant cardiac hypertrophy, measured using echocardiography to determine the diastolic interventricular septum thickness (Fig. 7*B*). Echocardiography of mice subjected to AAC revealed no change in left ventricular systolic function (measured by the percentage of fractional shortening of the left ventricle) compared with sham-operated animals (Fig. 7*C*).

BP, heart rate, and the development of cardiac hypertrophy in VASP knockout mice. As shown in Fig. 9, *A* and *B*, $VASP^{null}$ and $VASP^{+/+}$ mice had similar basal BP and resting heart rate. To explore the role that VASP plays in the stressed heart, we subjected mice lacking VASP to TAC, which subacutely in-

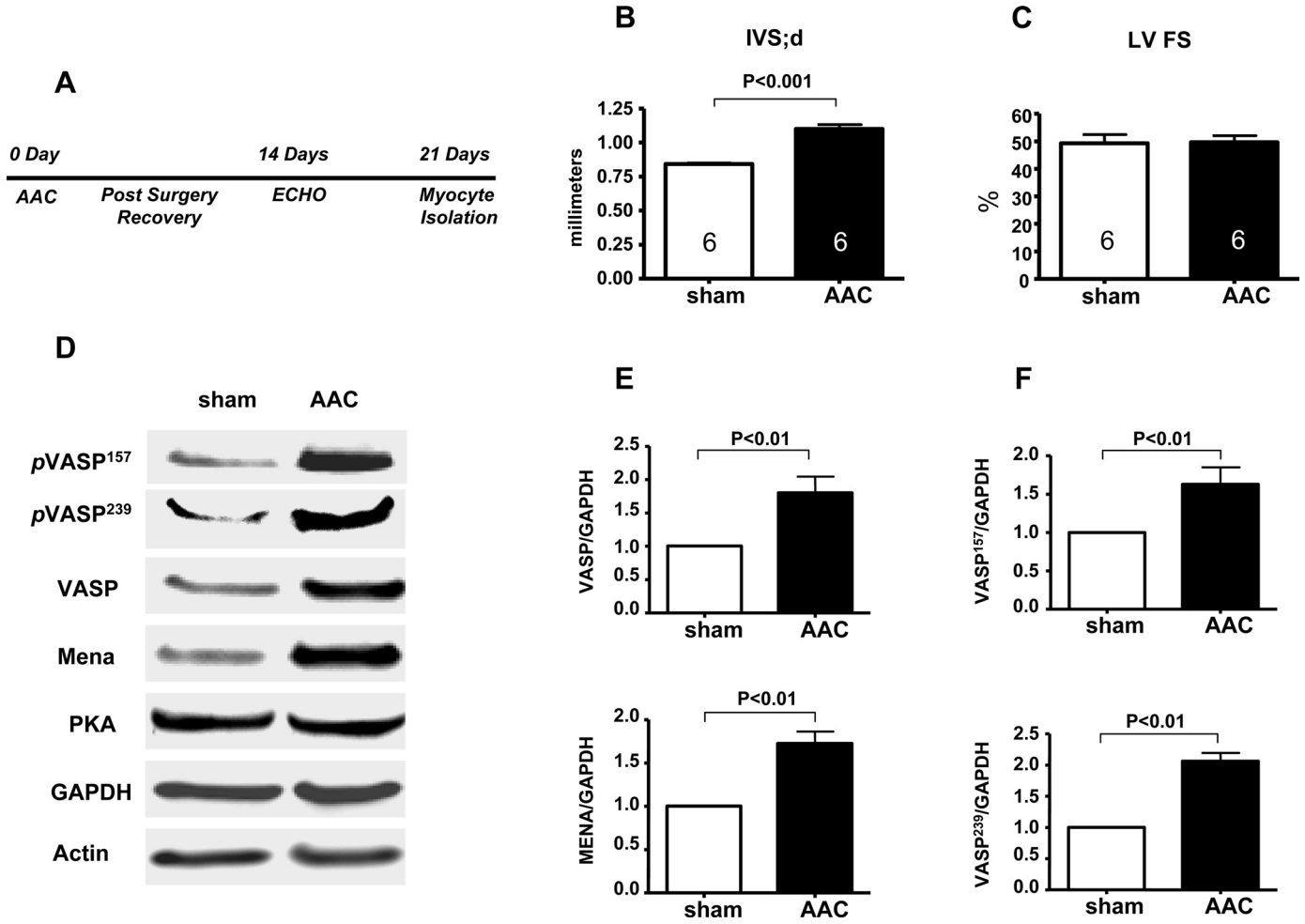

Fig. 7. MENA (mammalian homolog of Enabled)/VASP expression and VASP phosphorylation in cardiac myocytes isolated from hypertrophic hearts. This figure shows results of immunoblots analyzed in lysates prepared from cardiac myocytes isolated from mice subjected to ascending aortic constriction (AAC) or sham-operated mice. *A*: the time line from AAC surgery to cardiac myocyte isolation. *B* and *C*: echocardiographic analyses from AAC and sham-operated mice, including diastolic interventricular septal thickness (IVS-d; *B*) and left ventricular fractional shortening (LV-FS; *C*). *D*: cell lysates were resolved by SDS-PAGE and probed using antibodies directed against pVASP Ser157, pVASP Ser239, total VASP, MENA, actin, GAPDH, and PKA, as indicated. The experiment is representative of six independent experiments that yielded similar results. *E*: results of densitometric analyses from pooled data, plotting the total VASP or MENA abundance relative to GAPDH abundance. *F*: results of densitometric analyses from pooled data, plotting the pVASP Ser157 or Ser239 abundance relative to GAPDH abundance. Each data point represents the mean ± SE derived from six independent experiments (*t*-test). The number of mice per group is shown inside bars of *B* and *C*.

creases the workload on the heart. As shown in Fig. 9*D*, mice subjected to TAC, both $VASP^{null}$ and $VASP^{+/+}$ mice, developed cardiac hypertrophy 5 wk after surgery, without a significant decrement in cardiac systolic function (Fig. 9*E*). There was no substantive change in cardiac myocyte morphology between $VASP^{null}$ and $VASP^{+/+}$ mice (Fig. 9*F*).

DISCUSSION

These studies have used a combination of pharmacological, biochemical, and genetic approaches to explore VASP phosphorylation pathways in adult murine cardiac myocytes. We found that β-adrenergic receptor activation by isoproterenol rapidly leads to VASP phosphorylation at Ser157 and Ser239 (Fig. 1). Several lines of evidence in this study implicate cAMP-dependent signaling pathways as the principal mechanism modulating isoproterenol-induced phosphorylation of VASP at both sites in adult cardiac myocytes. Treatment of cardiac myocytes with either the cAMP analog 8-CPT-cAMP-AM or with the adenylate cyclase activator forskolin results in a pattern of VASP phosphorylation at Ser157 and Ser239 that is identical to the phosphorylation response seen with isoproterenol (Fig. 2, *A–D*). Inhibition of PKA by compound H-89 abrogates isoproterenol-induced phosphorylation of VASP at Ser157 and Ser239 (Fig. 2, *E* and *F*). The nonselective PDE inhibitor IBMX, but not the PDE-5-selective inhibitor sildenafil, promotes an increase in VASP phosphorylation (Fig. 2, *G* and *H*). In the presence of IBMX, addition of isoproterenol yields no additional VASP phosphorylation, suggesting that cyclic nucleotide PDEs, but not PDE-5, may play a role in modulating VASP phosphorylation. Taken all together, these observations strongly implicate the β-adrenergic receptor/adenylate cyclase/cAMP/PKA pathway as the principal signaling system modulating the isoproterenol-induced phosphorylation of VASP at Ser157 and Ser239. We note that the immunoblots in this figure and throughout this paper reveal an apparent decrease in total VASP abundance following

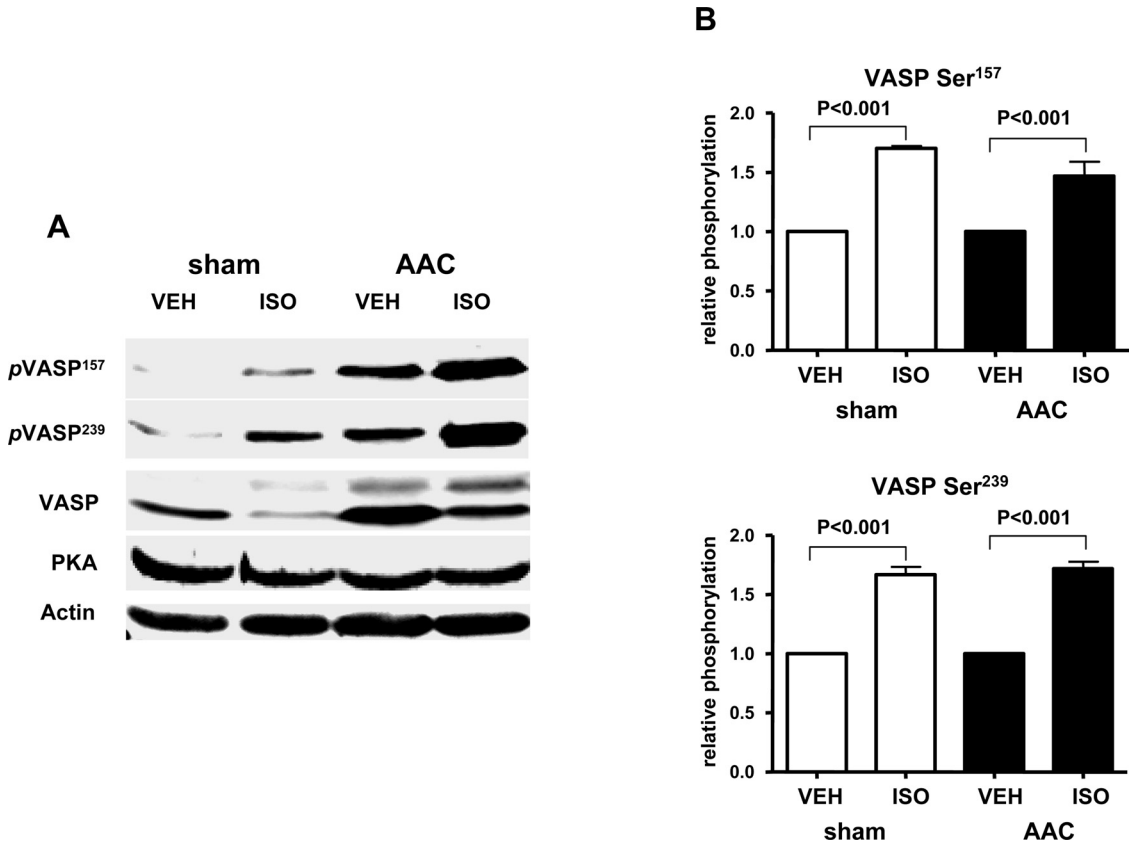

Fig. 8. ISO-induced VASP phosphorylation in cardiac myocytes isolated from hypertrophic hearts. This figure shows results of immunoblots analyzed in lysates prepared from cardiac myocytes isolated from mice subjected to AAC or sham-operated mice treated with ISO (100 nM for 5 min). *A*: cell lysates were resolved by SDS-PAGE and probed using antibodies directed against pVASP Ser157, pVASP Ser239, total VASP, actin, or PKA, as indicated. The experiment is representative of four independent experiments that yielded similar results. *B*: results of densitometric analyses from pooled data, plotting the fold increase in pVASP Ser157 or Ser239 relative to the signals present in untreated cells. Each data point represents the mean ± SE derived from four independent experiments (ANOVA).

treatments with isoproterenol or other agonists that enhance VASP Ser157 phosphorylation. We interpret this decreased protein signal as reflecting a change in the apparent M_r of VASP as a consequence of its phosphorylation (17): for reasons that remain poorly understood, protein phosphorylation is often accompanied by slower mobility on SDS-PAGE and sometimes (as appears to be the case for VASP) with a change in antigenicity. The transient decrease in the immunoblotted VASP signal following isoproterenol treatment appears to be a consequence of VASP Ser157 phosphorylation, leading to slower migration on SDS-PAGE, and also associated with a decreased affinity of the antibody for the phosphorylated protein.

A different pattern of VASP phosphorylation is seen following activation of cGMP-dependent pathways (Fig. 5). Murine cardiac myocytes are characterized by two distinct guanylate cyclase signaling pathways: the sGC, which is directly activated by NO, and the membrane-associated particulate guanylate cyclase, which is directly activated by ANP. NO in cardiac myocytes can be synthesized by either the endothelial isoform of NOS (eNOS) or by the nNOS isoform, both of which are expressed in these cells. Although the receptor-modulated pathways controlling nNOS activation in cardiac cells are less extensively characterized, we and others have clearly established that isoproterenol treatment of cardiac myocytes leads to the phosphorylation (Fig. 3) and activation of eNOS (3, 22). However, in the present studies, using both pharmacological and genetic approaches, we do not find evidence for the direct involvement of cardiac NOS pathways in modulating isoproterenol-induced VASP phosphorylation. We found that inhibition of NOS in cardiac myocytes by the NOS inhibitor L-NAME failed entirely to block VASP phosphorylation (Fig. 3, *C* and *D*). Basal as well as isoproterenol-promoted VASP phosphorylation was unchanged in cardiac myocytes isolated from $eNOS^{-/-}$ or $nNOS^{-/-}$ mice, arguing against a central role for endogenous NOS isoforms in control of VASP phosphorylation. Inhibition of sGC in these cells using the selective inhibitor ODQ similarly showed no significant effect on isoproterenol-modulated VASP phosphorylation (Fig. 3, *E* and *F*). These two lines of evidence point away from a central role for cardiac myocyte NOS-cGMP pathways in isoproterenol-mediated VASP phosphorylation and are consistent with our finding that β-adrenergic receptor-dependent VASP phosphorylation is entirely unchanged in cardiac myocytes isolated from $nNOS^{null}$ and $eNOS^{null}$ mice (Fig. 4). While it is formally possible that the eNOS and nNOS isoforms can compensate for one another when one or the other isoform is inactivated by gene targeting, this explanation seems less plausible, since neither NOS inhibition nor sGC inhibition affects the isoproterenol response (Fig. 3, *C–F*). Both eNOS

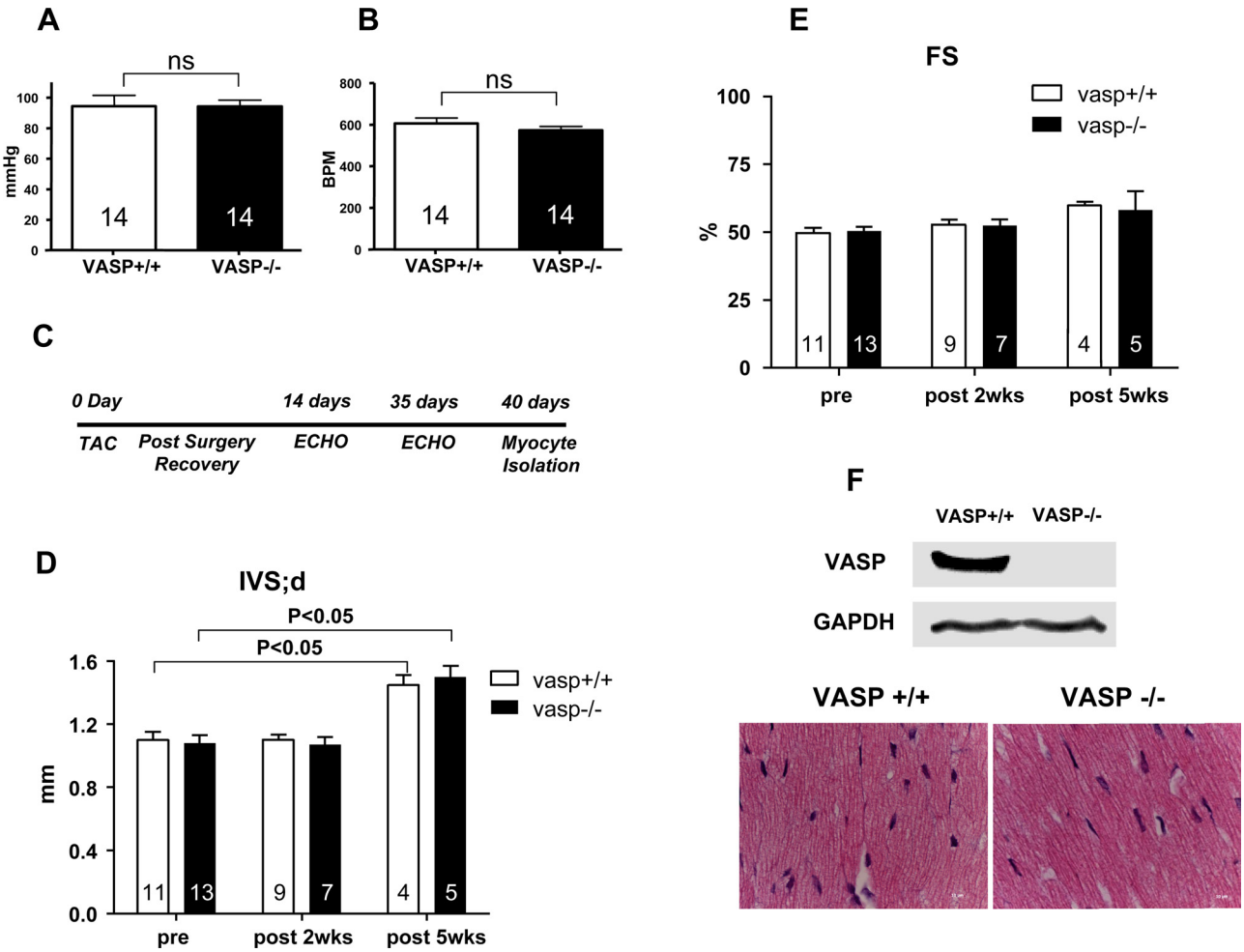

Fig. 9. Blood pressure, heart rate, and development of cardiac hypertrophy induced by transverse aortic constriction (TAC) in VASP$^{+/+}$ and VASP^{null} mice. *A* and *B*: basal mean blood pressure and basal heart rate in awake VASP$^{+/+}$ and VASP^{null} mice, respectively. *C*: the time line from TAC surgery to the two-dimensional echocardiogram analyses and cardiac myocyte isolation. *D* and *E*: echocardiographic parameters measured in TAC mice 2 wk before surgery (pre); 2 wk postsurgery (post 2 wks); and 5 wk postsurgery (post 5 wks). IVS-d (*D*) and LV FS (*E*) are shown. *F*: the results of immunoblots analyzed in lysates and hematoxylin/eosin staining of representative cross sections of cardiac myocytes from VASP$^{+/+}$ and VASP^{null} mice. Cell lysates were resolved by SDS-PAGE and probed using antibodies directed against total VASP and GAPDH, as indicated. Each data point represents the mean ± SE (ANOVA). The number of mice per group is shown inside the bars. BPM, heart rate in beats per minute.

and nNOS isoforms are constitutively expressed in cardiac myocytes, with some evidence that the endothelial and neuronal isoforms are localized to distinct subcellular compartment and have differential roles in cell signaling (11, 28, 41). eNOS is also robustly expressed in the vascular endothelial cells in the heart (11), and thus eNOS may play both an autocrine, as well as paracrine role in modulation of cardiac myocyte function. In contrast to the apparent lack of involvement of the endogenous NOS-sGC pathway in VASP phosphorylation, our experiments with ANP indicate that the particulate guanylate cyclase plays a role in VASP phosphorylation, albeit solely at Ser239, the site preferentially phosphorylated by the cGMP-dependent protein kinase (PKG). ANP does not promote VASP phosphorylation at Ser156, the site preferentially phosphorylated by PKA.

In contrast to the lack of involvement of cardiac myocyte NOS isoforms in modulating isoproterenol-induced VASP phosphorylation, we found that the NO-donating drug SNP stimulated VASP phosphorylation in these cells. As shown in Fig. 5, *A–C*, addition of SNP to adult murine cardiac myocytes leads to a prompt and reversible increase in VASP phosphorylation at Ser239. In contrast to the effect of isoproterenol, SNP produces no increase in phosphorylation of VASP at Ser157. Phospho-VASP Ser239 is known to be the site preferentially phosphorylated by PKG (38), although both PKA and PKG can phosphorylate VASP at either site under some experimental conditions (6). Importantly, the SNP-induced increase in phospho-VASP Ser239 is completely blocked by the sGC inhibitor ODQ (Fig. 5*C*). This observation stands in marked contrast to the complete failure of ODQ to attenuate isoproterenol-induced VASP phosphorylation responses (Fig. 3, *E* and *F*). Taken together, these results suggest that exogenous but not endogenous sources of NO promote the sGC-dependent phosphorylation of VASP. At least part of the explanation of this apparent paradox may derive from the fact that eNOS and nNOS have highly restricted and distinct subcellular localizations in cardiac myocytes. eNOS is localized to caveolin-1-enriched cardiac myocyte T-tubules (11), whereas nNOS appears to be strictly segregated in the endoplasmic reticulum (41). By contrast, extracellular or pharma-

cological sources of NO may be far more promiscuous in their cellular distribution (28). It seems quite plausible that eNOS, when localized in the vascular endothelium of cardiac blood vessels, or perhaps nNOS, located in cardiac nerve terminals, might play an important role in VASP modulation, even if these signaling enzymes, when expressed within purified cardiac myocytes, have little role in regulation of VASP. The spatial restriction of eNOS and nNOS to discrete subcellular locales may undermine these enzymes' ability to activate sGC, whereas pharmacological NO donors, such as SNP, or paracrine sources of NO may not be limited by these spatial constraints and thus are able to robustly activate sGC in these cells. These results further suggest that modulation of VASP phosphorylation by NO represents a paracrine rather an autocrine response, as is the case for many other NO-dependent signaling pathways. For example, VASP represents a target of endothelial cell-derived NO in the paracrine activation of sGC/PKG pathways that are located in vascular smooth muscle cells.

An important role for guanylate cyclases in VASP phosphorylation in cardiac myocytes is further established in experiments using the heart-derived peptide ANP (Fig. 5, *D* and *E*). ANP binds to and activates the particulate guanylate cyclase in target tissues, including cardiac myocytes, leading to striking increases in intracellular levels of cGMP in several cardiovascular tissues (25, 32). As we found for SNP, ANP promotes reversible phosphorylation of VASP at Ser239 in cardiac myocytes, without affecting Ser157 phosphorylation. The response to ANP is unaffected by the sGC inhibitor ODQ (data not shown), consistent with ANP's known role in activation of the particulate guanylate cyclase, but not sGC (25). Additionally, activation of cGMP-dependent protein kinases by 8-bromo-cGMP or activation of adenylate cyclase by forskolin (Fig. 5*F*) further confirms the distinguished substrate specificity of cardiac VASP phosphorylation at Ser239 by cGMP and the indiscriminate specificity of cAMP as a substrate for both sites, Ser157 and Ser239.

These studies have established that the cardiac signaling pathways that modulate cyclic nucleotide responses also importantly influence VASP phosphorylation in cardiac myocytes. Some of these same signaling pathways are implicated in cardiac disease states. For example, ANP levels increase strikingly in heart failure, and the NO/cGMP pathway has been shown to attenuate hypertrophic responses in cardiac myocytes. In addition, the activation of adrenergic responses has been shown to accompany the development of heart failure. However, the role (if any) of VASP phosphorylations in cardiac pathophysiology is unknown. VASP has the ability to bind cytoskeletal proteins and regulate actin cytoskeleton dynamics (18, 26). Because diabetic cardiomyopathy involves pathological changes in cardiac actin cytoskeleton following left ventricular remodeling and loss of intracellular contacts (9, 31, 37), we decided to explore VASP expression and phosphorylation patterns in cardiac myocytes isolated from diabetic mice. Cardiomyocytes from diabetic heart had no change in total VASP expression (Fig. 6, *A* and *B*), nor in the abundance of PKA (Fig. 6*A*). However, we found a significant increase in basal VASP phosphorylation at both Ser157 and Ser239 sites (Fig. 6*C*). In cardiac myocytes isolated from *db/db* obese diabetic mice, there was no significant additional response to isoproterenol treatment on top of the augmented basal VASP phosphorylation already seen in these cells. However, inhibition of PKA with compound H-89 entirely abrogates the increased level of VASP phosphorylation at both Ser157 and Ser239, again demonstrating that the PKA pathway is a key determinant of phosphorylation responses at both sites.

Cardiovascular disease is the most common complication of diabetes (14). Murine models of diabetes, including the *db/db* obese diabetic mouse that was analyzed in the present studies, show evidence of cardiomyopathy associated with metabolic perturbations in cardiac myocytes, which occur independently of myocardial ischemia (reviewed in Ref. 1). We found no change in VASP expression in cardiac myocytes isolated from *db/db* mice, but basal VASP phosphorylation was increased (Fig. 6). VASP phosphorylation modulates actin dynamics (26), and it is plausible that the enhanced levels of phosphorylated VASP seen in myocytes from in both *db/db* diabetic (Fig. 6) and hypertrophic models (Figs. 7 and 8) may reflect the cytoskeletal remodeling that accompanies the transition to heart failure (27). There is no substantive alteration in the subtle insulin- or ANP-stimulated phosphorylation of VASP at Ser239 in cardiocytes isolated from *db/db* diabetic mice, nor is the robust insulin-dependent activation of kinase Akt altered in cardiac myocytes from diabetic mice. These findings suggest that insulin and ANP signaling to PKG is not significantly affected in the *db/db* model; the insulin-Akt axis is likewise unperturbed.

Because cardiomyopathy with systolic and diastolic dysfunction is evident in diabetic *db/db* mice (1, 36), we extended our work to analyze MENA/VASP expression and agonist-modulated VASP phosphorylation in cardiac myocytes isolated from hypertrophic hearts from mice subjected to AAC. The models of cardiac hypertrophy induced by AAC (Figs. 7 and 8) and TAC (Fig. 9) differ in their hemodynamic consequences and in the time course to development of heart failure. Cardiocytes from mice subjected to AAC show an increase in overall VASP abundance, with a corresponding increase in the absolute level of phosphorylated VASP. When the increase in phosphorylated VASP in cardiocytes is normalized to the increased level of total VASP expression seen following aortic constriction, the relative level of VASP phosphorylation is unchanged. It is notable that overall VASP phosphorylation is increased in cardiocytes isolated either from the *db/db* diabetic mouse or following AAC. Unfortunately, none of the commercially available VASP antibodies were found to yield a convincing signal in immunohistochemical studies of heart tissue (data not shown), despite the robust VASP expression documented in immunoblot analyses of isolated cardiocytes. Nonetheless, since VASP phosphorylation modulates actin assembly (28), it seems plausible that the absolute increase in the abundance of phosphorylated VASP may play a role in cytoskeletal remodeling in these mouse models of cardiac dysfunction.

The pathological cardiac phenotype that was previously documented in transgenic mice expressing a dominant-negative form of VASP pointed to a possible role for VASP in the modulation of cardiac cell shape and/or in ventricular remodeling (10). However, our initial findings in VASP^{null} mice failed to document a distinctive cardiac phenotype for these mice, perhaps suggesting that expression of this protein is not required for normal cardiovascular function (19). VASP has been considered as a candidate "modifier gene" that affects the

response of heart to pressure overload or other stress conditions (5). To address the hypothesis of VASP as a modifier gene that could affect cardiac function under stress conditions, age-matched wild-type and VASP^{null} mice underwent surgical aortic constriction, and cardiac function was evaluated in vivo by using two-dimensional echocardiography over the ensuing 5 wk. These studies did not identify a critical role for VASP during the increased hemodynamic load in the heart following aortic constriction (Fig. 9), in both cases showing hypertrophy without evident heart failure. Longer term studies of these and other models of cardiac hypertrophy and heart failure will be required to delineate the myocardial remodeling pathways regulated by VASP. It remains possible that VASP plays a key role in other pathophysiological processes in the heart. These studies have found that not only is VASP robustly expressed in cardiac myocytes (Fig. 7*D*) but also MENA, the second prominent member of the Ena/VASP-protein family. The colocalization of these two proteins has been found in many mouse tissues and suggests that these proteins may have similar overlapping functions; previous studies have suggested that VASP and MENA might be able to compensate for each other following knockout of one or the other gene (12, 19, 34). It is possible that the lack of a cardiac phenotype seen in the VASP^{null} mouse may reflect functional compensation by MENA. These studies do not determine whether the increased expression of MENA and VASP, in association with augmented VASP phosphorylation in hypertrophic heart, modulates or reflects a marker for hypertrophy or cardiac dysfunction in these mice, or whether VASP modulation might instead have a causal role. Further studies into the role and regulation of VASP and MENA in cardiac myocytes may provide new insights into the pathways controlling myocardial function in normal and diseased heart.

ACKNOWLEDGMENTS

We thank Drs. Ruqin Kou, Gordon Li, and Toru Sugiyama for helpful discussions and constructive critiques. We also thank Alex Loscalzo and Soeun Ngoy for excellent technical support.

GRANTS

The work was supported in part by National Institutes of Health Grants HL46457, HL48743, and GM36259 (to T. Michel), HL088533, HL093148, HL090884, and HL 071775 (to R. Liao), and by an American Diabetes Association/Takeda Cardiovascular Postdoctoral Fellowship Award (to J. L. Sartoretto).

REFERENCES

1. **An D, Rodriguez B.** Role of changes in cardiac metabolism in development of diabetic cardiomyopathy. *Am J Physiol Heart Circ Physiol* 291: H1489–H1506, 2006.
2. **Aszodi A, Pfeifer A, Ahmad M, Glauner M, Zhou XH, Ny L, Andersson KE, Kehrel B, Offermanns S, Fassler R.** The vasodilator-stimulated phosphoprotein (VASP) is involved in cGMP- and cAMP-mediated inhibition of agonist-induced platelet aggregation, but is dispensable for smooth muscle function. *EMBO J* 18: 37–48, 1999.
3. **Belhassen L, Feron O, Kaye DM, Michel T, Kelly RA.** Regulation by cAMP of post-translational processing and subcellular targeting of endothelial nitric-oxide synthase (type 3) in cardiac myocytes. *J Biol Chem* 272: 11198–11204, 1997.
4. **Blume C, Benz PM, Walter U, Ha J, Kemp BE, Renne T.** AMP-activated protein kinase impairs endothelial actin cytoskeleton assembly by phosphorylating vasodilator-stimulated phosphoprotein. *J Biol Chem* 282: 4601–4612, 2007.
5. **Brancaccio M, Hirsch E, Notte A, Selvetella G, Lembo G, Tarone G.** Integrin signalling: the tug-of-war in heart hypertrophy. *Cardiovasc Res* 70: 422–433, 2006.
6. **Butt E, Abel K, Krieger M, Palm D, Hoppe V, Hoppe J, Walter U.** cAMP- and cGMP-dependent protein kinase phosphorylation sites of the focal adhesion vasodilator-stimulated phosphoprotein (VASP) in vitro and in intact human platelets. *J Biol Chem* 269: 14509–14517, 1994.
7. **Chen H, Levine YC, Golan DE, Michel T, Lin AJ.** Atrial natriuretic peptide-initiated cGMP pathways regulate vasodilator-stimulated phosphoprotein phosphorylation and angiogenesis in vascular endothelium. *J Biol Chem* 283: 4439–4447, 2008.
8. **Comerford KM, Lawrence DW, Synnestvedt K, Levi BP, Colgan SP.** Role of vasodilator-stimulated phosphoprotein in PKA-induced changes in endothelial junctional permeability. *FASEB J* 16: 583–585, 2002.
9. **Dyntar D, Sergeev P, Klisic J, Ambuhl P, Schaub MC, Donath MY.** High glucose alters cardiomyocyte contacts and inhibits myofibrillar formation. *J Clin Endocrinol Metab* 91: 1961–1967, 2006.
10. **Eigenthaler M, Engelhardt S, Schinke B, Kobsar A, Schmitteckert E, Gambaryan S, Engelhardt CM, Krenn V, Eliava M, Jarchau T, Lohse MJ, Walter U, Hein L.** Disruption of cardiac Ena-VASP protein localization in intercalated disks causes dilated cardiomyopathy. *Am J Physiol Heart Circ Physiol* 285: H2471–H2481, 2003.
11. **Feron O, Belhassen L, Kobzik L, Smith TW, Kelly RA, Michel T.** Endothelial nitric oxide synthase targeting to caveolae. Specific interactions with caveolin isoforms in cardiac myocytes and endothelial cells. *J Biol Chem* 271: 22810–22814, 1996.
12. **Gambaryan S, Hauser W, Kobsar A, Glazova M, Walter U.** Distribution, cellular localization, and postnatal development of VASP and Mena expression in mouse tissues. *Histochem Cell Biol* 116: 535–543, 2001.
13. **Gertler FB, Niebuhr K, Reinhard M, Wehland J, Soriano P.** Mena, a relative of VASP and Drosophila Enabled, is implicated in the control of microfilament dynamics. *Cell* 87: 227–239, 1996.
14. **Haffner SM, Lehto S, Ronnemaa T, Pyorala K, Laakso M.** Mortality from coronary heart disease in subjects with type 2 diabetes and in nondiabetic subjects with and without prior myocardial infarction. *N Engl J Med* 339: 229–234, 1998.
15. **Halbrugge M, Walter U.** Analysis, purification and properties of a 50,000-dalton membrane-associated phosphoprotein from human platelets. *J Chromatogr* 521: 335–343, 1990.
16. **Halbrugge M, Walter U.** Purification of a vasodilator-regulated phosphoprotein from human platelets. *Eur J Biochem* 185: 41–50, 1989.
17. **Hamad AM, Clayton A, Islam B, Knox AJ.** Guanylyl cyclases, nitric oxide, natriuretic peptides, and airway smooth muscle function. *Am J Physiol Lung Cell Mol Physiol* 285: L973–L983, 2003.
18. **Harbeck B, Huttelmaier S, Schluter K, Jockusch BM, Illenberger S.** Phosphorylation of the vasodilator-stimulated phosphoprotein regulates its interaction with actin. *J Biol Chem* 275: 30817–30825, 2000.
19. **Hauser W, Knobeloch KP, Eigenthaler M, Gambaryan S, Krenn V, Geiger J, Glazova M, Rohde E, Horak I, Walter U, Zimmer M.** Megakaryocyte hyperplasia and enhanced agonist-induced platelet activation in vasodilator-stimulated phosphoprotein knockout mice. *Proc Natl Acad Sci USA* 96: 8120–8125, 1999.
20. **Hein S, Kostin S, Heling A, Maeno Y, Schaper J.** The role of the cytoskeleton in heart failure. *Cardiovasc Res* 45: 273–278, 2000.
21. **Heling A, Zimmermann R, Kostin S, Maeno Y, Hein S, Devaux B, Bauer E, Klovekorn WP, Schlepper M, Schaper W, Schaper J.** Increased expression of cytoskeletal, linkage, and extracellular proteins in failing human myocardium. *Circ Res* 86: 846–853, 2000.
22. **Kanai AJ, Mesaros S, Finkel MS, Oddis CV, Birder LA, Malinski T.** Beta-adrenergic regulation of constitutive nitric oxide synthase in cardiac myocytes. *Am J Physiol Cell Physiol* 273: C1371–C1377, 1997.
23. **Kass DA, Champion HC, Beavo JA.** Phosphodiesterase type 5: expanding roles in cardiovascular regulation. *Circ Res* 101: 1084–1095, 2007.
24. **Kass DA, Takimoto E, Nagayama T, Champion HC.** Phosphodiesterase regulation of nitric oxide signaling. *Cardiovasc Res* 75: 303–314, 2007.
25. **Kato T, Muraski J, Chen Y, Tsujita Y, Wall J, Glembotski CC, Schaefer E, Beckerle M, Sussman MA.** Atrial natriuretic peptide promotes cardiomyocyte survival by cGMP-dependent nuclear accumulation of zyxin and Akt. *J Clin Invest* 115: 2716–2730, 2005.
26. **Krause M, Dent EW, Bear JE, Loureiro JJ, Gertler FB.** Ena/VASP proteins: regulators of the actin cytoskeleton and cell migration. *Annu Rev Cell Dev Biol* 19: 541–564, 2003.
27. **Lindsey ML, Yoshioka J, MacGillivray C, Muangman S, Gannon J, Verghese A, Aikawa M, Libby P, Krane SM, Lee RT.** Effect of a cleavage-resistant collagen mutation on left ventricular remodeling. *Circ Res* 93: 238–245, 2003.

28. **Michel T.** Nitric oxide synthase 3. *UCSD-Nature Molecule Pages.* doi:10.1038/mp.a001660.01.
29. **Molenaar P, Parsonage WA.** Fundamental considerations of beta-adrenoceptor subtypes in human heart failure. *Trends Pharmacol Sci* 26: 368–375, 2005.
30. **Munzel T, Feil R, Mulsch A, Lohmann SM, Hofmann F, Walter U.** Physiology and pathophysiology of vascular signaling controlled by guanosine 3′,5′-cyclic monophosphate-dependent protein kinase [corrected]. *Circulation* 108: 2172–2183, 2003.
31. **Nemoto O, Kawaguchi M, Yaoita H, Miyake K, Maehara K, Maruyama Y.** Left ventricular dysfunction and remodeling in streptozotocin-induced diabetic rats. *Circ J* 70: 327–334, 2006.
32. **Nishikimi T, Maeda N, Matsuoka H.** The role of natriuretic peptides in cardioprotection. *Cardiovasc Res* 69: 318–328, 2006.
33. **O'Connell TD, Rodrigo MC, Simpson PC.** Isolation and culture of adult mouse cardiac myocytes. *Methods Mol Biol* 357: 271–296, 2007.
34. **Reinhard M, Jarchau T, Walter U.** Actin-based motility: stop and go with Ena/VASP proteins. *Trends Biochem Sci* 26: 243–249, 2001.
35. **Sakai K, Akima M, Tsuyama K.** Evaluation of the isolated perfused heart of mice, with special reference to vasoconstriction caused by intracoronary acetylcholine. *J Pharmacol Methods* 10: 263–270, 1983.
36. **Semeniuk LM, Kryski AJ, Severson DL.** Echocardiographic assessment of cardiac function in diabetic *db/db* and transgenic db/db-hGLUT4 mice. *Am J Physiol Heart Circ Physiol* 283: H976–H982, 2002.
37. **Shimoni Y, Rattner JB.** Type 1 diabetes leads to cytoskeleton changes that are reflected in insulin action on rat cardiac K(+) currents. *Am J Physiol Endocrinol Metab* 281: E575–E585, 2001.
38. **Smolenski A, Bachmann C, Reinhard K, Honig-Liedl P, Jarchau T, Hoschuetzky H, Walter U.** Analysis and regulation of vasodilator-stimulated phosphoprotein serine 239 phosphorylation in vitro and in intact cells using a phosphospecific monoclonal antibody. *J Biol Chem* 273: 20029–20035, 1998.
39. **Smolenski A, Poller W, Walter U, Lohmann SM.** Regulation of human endothelial cell focal adhesion sites and migration by cGMP-dependent protein kinase I. *J Biol Chem* 275: 25723–25732, 2000.
40. **Walter U, Eigenthaler M, Geiger J, Reinhard M.** Role of cyclic nucleotide-dependent protein kinases and their common substrate VASP in the regulation of human platelets. *Adv Exp Med Biol* 344: 237–249, 1993.
41. **Xu KY, Huso DL, Dawson TM, Bredt DS, Becker LC.** Nitric oxide synthase in cardiac sarcoplasmic reticulum. *Proc Natl Acad Sci USA* 96: 657–662, 1999.